competition between patches of microbes based on investment in toxin production. When we considered the first 14 days of the experiment, changes in relatedness tracked the changes in frequency of toxin producers, as might be expected from standard definitions of relatedness (supplementary materials), so that treatments with initially low frequencies of toxin producers had higher relatedness at time point 14 (treatments 0 and 0.05, Fig. 4, frequency*time interaction, likelihood ratio = 22.6, $P < 0.0001$). However, despite the rapid turnover in microbial populations at the plant level and wide fluctuation in the frequency of toxin producers between time points, relatedness at the level of the entire field plot remained high throughout the experiment (Fig. 4B). The highly aggregated distribution of bacteria on growing leaf tissue (supplementary materials and supplementary text) provides indirect support for our hypothesis of rare colonization. Evidence of the benefits of toxin production for local bacterial populations was found in the correlation between toxin production and bacterial density in the final time point of the field experiment (fig. S5; supplementary materials and supplementary text).

These experiments illustrate how cooperative, virulent bacteria and avirulent cheats compete and coexist in a natural environment. As social evolutionary theory predicts, nonproducing cheats can outcompete producers both within hosts and within local populations. Here, we have shown that cooperation can still be stable, because cheats drive down population density, and because cooperators do better when rare (negative frequency dependence) and at low population densities (negative density dependence). The rapidity with which toxin cheats can invade patches of cooperators is likely to have consequences for bacterial population dynamics. *B. thuringiensis*, unlike most insect pathogens, very rarely causes epidemics in the field (*27, 28*). The increased fitness of cheats at high densities and their ready availability in the soil mean that invasion of noninfectious cheats could rapidly curtail the direct host-host transmission required for an epidemic. In the field, *B. thuringiensis*–killed cadavers tend to fall into the soil soon after death (*22*), which suggests that most natural infections will occur indirectly after dispersal from a soil reservoir rather than from cadaver to larva during epidemics.

The more general implications of this work will depend on the prevalence of cooperative virulence among bacterial pathogens. However, a large number of essential virulence factors in important human pathogens are likely to be cooperative because they are exotoxins, which are necessarily secreted outside of the bacterial cell and are therefore potentially exploitable by cheats. These include anthrax toxins, diptheria toxin, cholera toxin, Shiga toxin, *Clostridium* spp. exotoxins, pneumolysin, botulinum toxin, pertussis toxin, *Staphylococcus* alpha toxin, and tetanus toxin (*29*). In some instances (e.g., in

Vibrio cholerae) the ecological similarities with *B. thuringiensis* are striking; natural populations are composed of both toxin producers and nonproducers, toxin binding occurs on intestinal receptors and activates the release of host resources, and secreted toxins are encoded on mobile elements (*30*). Our results suggest that social interactions between toxin producers and nonproducers can explain the coexistence of virulent and avirulent bacteria and that sociality will influence the dynamics of virulence in natural populations.

References and Notes
1. S. A. West, A. S. Griffin, A. Gardner, S. P. Diggle, *Nat. Rev. Microbiol.* **4**, 597 (2006).
2. M. A. Brockhurst, M. E. Hochberg, T. Bell, A. Buckling, *Curr. Biol.* **16**, 2030 (2006).
3. S. P. Diggle, A. S. Griffin, G. S. Campbell, S. A. West, *Nature* **450**, 411 (2007).
4. S. A. West, A. Buckling, *Proc. R. Soc. Lond. B Biol. Sci.* **270**, 37 (2003).
5. J. L. Sachs, U. G. Mueller, T. P. Wilcox, J. J. Bull, *Q. Rev. Biol.* **79**, 135 (2004).
6. S. A. Frank, *Foundations of Social Evolution* (Princeton Univ. Press, Princeton, NJ, 1998).
7. S. P. Brown, *Proc. R. Soc. Lond. B Biol. Sci.* **266**, 1899 (1999).
8. A. S. Griffin, S. A. West, A. Buckling, *Nature* **430**, 1024 (2004).
9. K. M. Sandoz, S. M. Mitzimberg, M. Schuster, *Proc. Natl. Acad. Sci. U.S.A.* **104**, 15876 (2007).
10. S. P. Brown, M. E. Hochberg, B. T. Grenfell, *Trends Microbiol.* **10**, 401 (2002).
11. S. A. Frank, *Q. Rev. Biol.* **71**, 37 (1996).
12. A. Buckling, M. A. Brockhurst, *Heredity* **100**, 484 (2008).
13. J. E. Strassmann, Y. Zhu, D. C. Queller, *Nature* **408**, 965 (2000).
14. R. C. MacLean, I. Gudelj, *Nature* **441**, 498 (2006).
15. K. P. Rumbaugh *et al.*, *Curr. Biol.* **19**, 341 (2009).
16. T. Köhler, A. Buckling, C. van Delden, *Proc. Natl. Acad. Sci. U.S.A.* **106**, 6339 (2009).
17. A. Ross-Gillespie, A. Gardner, S. A. West, A. S. Griffin, *Am. Nat.* **170**, 331 (2007).
18. B. Raymond, P. R. Johnston, C. Nielsen-LeRoux, D. Lereclus, N. Crickmore, *Trends Microbiol.* **18**, 189 (2010).
19. M. Soberón *et al.*, *Science* **318**, 1640 (2007).
20. B. Raymond, S. L. Elliot, R. J. Ellis, *J. Invertebr. Pathol.* **98**, 307 (2008).
21. H. Agaisse, D. Lereclus, *J. Bacteriol.* **177**, 6027 (1995).
22. B. Raymond, K. L. Wyres, S. K. Sheppard, R. J. Ellis, M. B. Bonsall, *PLoS Pathog.* **6**, e1000905 (2010).
23. F. A. Collier, S. L. Elliot, R. J. Ellis, *FEMS Microbiol. Ecol.* **54**, 417 (2005).
24. Materials and methods are available as supplementary materials on *Science* Online.
25. W. D. Hamilton, *J. Theor. Biol.* **7**, 1 (1964).
26. O. M. Gilbert, K. R. Foster, N. J. Mehdiabadi, J. E. Strassmann, D. C. Queller, *Proc. Natl. Acad. Sci. U.S.A.* **104**, 8913 (2007).
27. M. Porcar, P. Caballero, *J. Appl. Microbiol.* **89**, 309 (2000).
28. J. Myers, *Adv. Ecol. Res* **18**, 179 (1988).
29. L. M. Prescott, J. P. Harley, D. A. Klein, *Microbiology* (McGraw-Hill, New York, ed. 5, 2002).
30. J. Reidl, K. E. Klose, *FEMS Microbiol. Rev.* **26**, 125 (2002).

A Single Promoter Inversion Switches *Photorhabdus* Between Pathogenic and Mutualistic States

Vishal S. Somvanshi,[1]* Rudolph E. Sloup,[1] Jason M. Crawford,[2]† Alexander R. Martin,[1] Anthony J. Heidt,[1] Kwi-suk Kim,[1] Jon Clardy,[2] Todd A. Ciche[1]‡

Microbial populations stochastically generate variants with strikingly different properties, such as virulence or avirulence and antibiotic tolerance or sensitivity. *Photorhabdus luminescens* bacteria have a variable life history in which they alternate between pathogens to a wide variety of insects and mutualists to their specific host nematodes. Here, we show that the *P. luminescens* pathogenic variant (P form) switches to a smaller-cell variant (M form) to initiate mutualism in host nematode intestines. A stochastic promoter inversion causes the switch between the two distinct forms. M-form cells are much smaller (one-seventh the volume), slower growing, and less bioluminescent than P-form cells; they are also avirulent and produce fewer secondary metabolites. Observations of form switching by individual cells in nematodes revealed that the M form persisted in maternal nematode intestines, were the first cells to colonize infective juvenile (IJ) offspring, and then switched to P form in the IJ intestine, which armed these nematodes for the next cycle of insect infection.

Pathogenic and mutualistic bacteria can exist in different states in their host to survive sudden environmental shifts such as antibiotic exposure or host immune activation (*1, 2*). *Photorhabdus luminescens* bacteria are

bioluminescent symbionts of *Heterorhabditis bacteriophora* nematodes, and the two organisms (as a mutualistic pair) infect, kill, and reproduce inside insects. Nematodes in the infective juvenile (IJ) stage penetrate an insect host and

regurgitate their intestinal symbionts in the insect hemocoel (*3*), which leads to the death of the insect and the release of nutrients that support nematode reproduction (*4*). Inside the insect, the bacteria grow exponentially and secrete potent Tc and Mcf insecticidal toxins (*5–7*). The symbionts also produce crystalline inclusion proteins (Cips) with high levels of essential amino acids that are required for nematode reproduction, as well as antimicrobials that defend the insect cadaver from microbial competitors (*8*, *9*). Nematode-bacterial associations were identified, and pulse-chase methodologies were performed (to limit symbionts) as described previously (*10*). The symbionts are maternally transmitted to IJ offspring developing inside the nematode's body (*10*). Mutualism is initiated when *Photorhabdus* phase variants express maternal adhesion (Mad) fimbriae and adhere to the nematode intestine (*11*). Fimbriae are proteinaceous surface filaments that function in bacterial cell adherence during host-cell colonization (*12*). Transmission proceeds through a series of steps involving adherence, invasion, and intracellular growth (*10*).
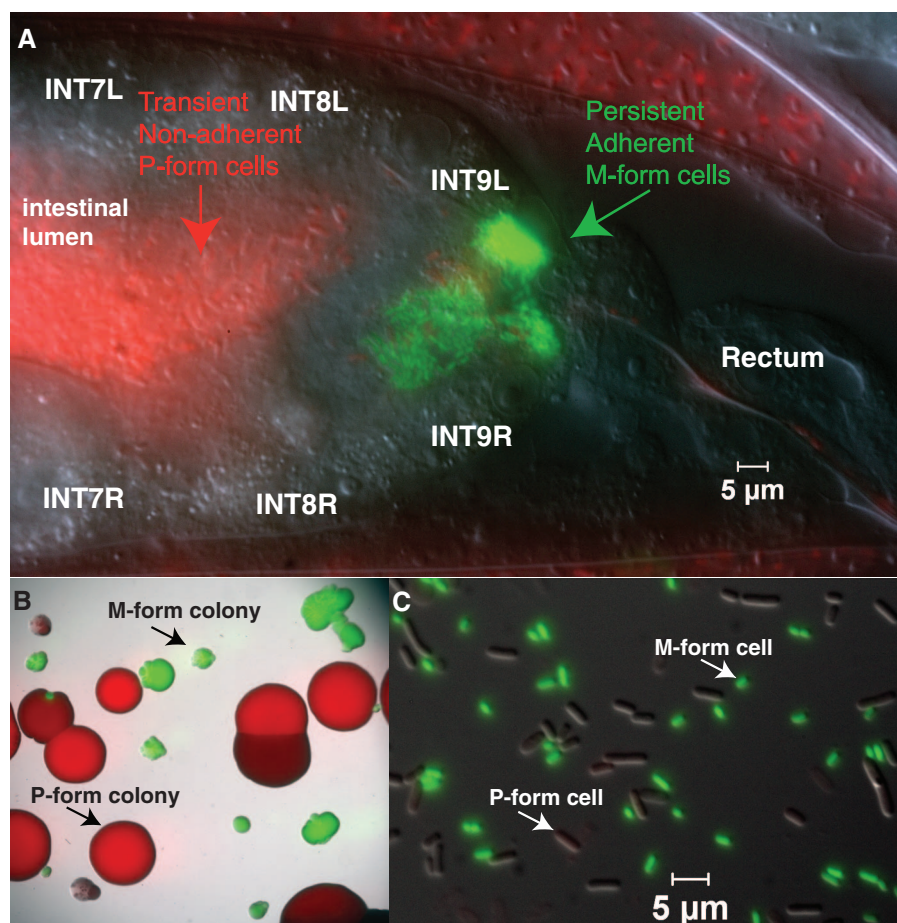
By visualizing individual cells inside nematode intestines, we discovered that *Photorhabdus* switched to a distinct small-cell form to initiate mutualism (M form), different from the insect pathogenic (P-form) cells that were only transiently present inside intestines (Fig. 1A and figs. S1 and S2). The M-form cells lacked visible CipA and CipB inclusions that were produced by the P form and are essential for nematode reproduction (*8*) (fig. S2). The M form grew as translucent small-colony variants (*13*) consisting of small cells, with opaque sectors of larger P-form cells irrupting after 48 hours and eventually dominating the colony (fig. S3). Before our observations, the biological significance of small-colony variants was unknown, and the P form was considered the "wild type" because it is the predominant form isolated from entomopathogenic nematodes and infected insects, and it produces the antibiotics, bioluminescence, Cips, and insecticidal toxins normally associated with *Photorhabdus* bacteria (*5–9*, *14*). Observing the development of this microbial symbiosis inside the nematodes revealed that the P form switches to the M form, which site-specifically colonizes the maternal nematode intestine to initiate mutualism.

Switching from P to M form correlated with promoter inversion from OFF to ON orientations and, consequently, the expression of the Mad fimbrial locus. This switch enabled a minority variant population to selectively adhere to the posterior maternal intestine (fig. S4) (*11*). Inversion of the *madswitch* promoter occurring between two 36–base pair (bp) inverted repeats flanking 257 bp (Fig. 2) regulates *mad*, in an ON or OFF type of phase variation (*15*, *16*). Cells stochastically express *mad*, which indicates that it is a highly mutable contingency locus (*1*). M-form cells transcribed *madA* from the *madswitch* when oriented ON and linked the M form with promoter inversion (fig. S4). We determined previously that P-form colonies aged up to 60 days in a Petri dish predominantly switched to the *madswitch* oriented ON (*11*). Viable cells isolated from these colonies then grew as the M form (fig. S5). However, the M form prevailed much sooner (4 days) in vivo after P-form infection of *Galleria mellonella* insect larvae, and this assay was subsequently used to examine form switching independent of mutualism (Fig. 2 and fig. S5). We developed a recombination methodology to manipulate the *Photorhabdus* genome (fig. S6). The original disruptions in *madA* and

madH predicted to encode the major subunit and usher-assembled fimbrial proteins, respectively, failed to generate the M form, which indicated that *mad* expression was required for M formation (Fig. 2). However, in-frame *madA* and *madH* deletion mutants still generated the M form, while retaining observable defects in nematode mutualism, including no detectable adhesion to the maternal nematode intestine or colonization of IJ nematodes. Taken together, these results suggest that the original mutations prevented M formation because of polarity on a distal regulator rather than on fimbriae structural genes.

One distal *mad* gene, *madJ*, was an attractive target as the possible cause of the M form because it encodes a homolog of CaiF (*17*) and of GrlA (*18*), transcriptional activators of enterohemorrhagic *Escherichia coli*. Deletion of *madJ* prevented M formation and severely compromised mutualism, which supported a functional role for MadJ as the regulatory output for M formation (Fig. 2, B and H, and Table 1). Half of the maternal nematodes associated with Δ*madJ* lacked detectable persistent bacteria; the other half had visibly fewer persistent bacteria and

[1]Department of Microbiology and Molecular Genetics and Center for Microbial Pathogenesis, Michigan State University, East Lansing, MI 48824, USA. [2]Department of Biological Chemistry and Molecular Pharmacology, Harvard Medical School, Boston, MA 02115, USA.

*Present address: Division of Biological Sciences, University of California, San Diego, La Jolla, CA 92093, USA.
†Present address: Department of Chemistry and Chemical Biology Institute, Yale University, New Haven, CT 06520, USA.
‡To whom correspondence should be addressed. E-mail: ciche@msu.edu

Fig. 1. *Photorhabdus* cells that initiate mutualism in the nematode intestine are small-cell variant M-form cells. (**A**) *Photorhabdus* cells that initiate mutualism (green) on the ninth intestinal ring cells, left and right, INT9L and INTR, posterior intestinal cells and transients (red) are present throughout the lumen of the nematode. (**B**) M-form cells develop small colonies, and transient P-form cells develop large colonies. (**C**) Small colonies consist of primarily small cells, and large colonies consist of primarily larger cells.

transmitted symbionts to only 21.5% of IJ progeny (Table 1). Attempts to complement the Δ*madJ* mutation by expressing *madJ* in trans from a broad host range plasmid were unsuccessful, because the plasmid was not maintained (see methods in the supplementary material). To further test the effect of *madswitch* inversion on mutualism and M formation, we deleted an invertase (i.e., a tyrosine-type site-specific recombinase) gene, *madR*, adjacent to the *madswitch*, but this failed to disrupt M formation or mutualism, which indicated that MadR is not involved in switching or that its function is redundant with another invertase that functions as the ON switch (Fig. 2, B and F). However, deleting a single orphan invertase gene, *madO* (*plu1991*), located 575 bp upstream of *fruB* (fig. S1), prevented M formation and mutualism (Fig. 2, B, G, and H, and Table 1), which indicated that MadO is required to switch the *madswitch* ON and to allow *madJ* expression. The expression levels of MadO could control the

rate of promoter inversion from OFF to ON, or other factors may limit switching.

To test the effects of *madswitch* promoter inversion on phenotype switching, we genetically locked the *madswitch* to either the ON or OFF orientation (fig. S7). The *madswitch* was locked ON and OFF by recombining the switch in either orientation while deleting the upstream inverted repeat and *madR* (fig. S7). The *madswitch* reporter was similarly constructed, which resulted in *madA*-FRT-*gfp*-*madB*. M formation was assayed by injecting P-form cells into *Galleria mellonella* larvae, and then 4 days later determining the percentage of M-form colonies. Deleting the upstream inverted repeat in P-form cells locked the *madswitch* OFF and prevented the locked (L)/P-form (which failed to initiate mutualism) from being transmitted to IJ nematodes; cells that switched to the M-form phenotype were not detected (Fig. 2, B and D, and Table 1). Conversely, deleting the same repeat while inverting the *madswitch* ON

switched the P form to L/M-form colonies without P-form sectors (Fig. 2, B and E; fig. S3; and Table 1). All recombinants had the L/M-form phenotype; several of these were frozen, and one was used for further study. The L/M form initiated mutualism and was transmitted to IJ nematode offspring (Fig. 2 D and E, and Table 1). Thus, the orientation of the *madswitch* promoter determines the phenotype and life-style of *Photorhabdus*.

Having locked M and P forms (fig. S7) enabled us to determine their many phenotypic differences. The M-form cells were shorter (length = 1.2 versus 4.4 μm), were smaller in diameter (0.8 versus 1.2 μm) and volume (0.7 versus 4.8 μm^3), and contained no visible Cips compared with the P form (fig. S3). The M form grew more slowly [μ = 0.09 ± 0.003 (SEM)] than the P form [μ = 0.13 ± 0.02 (SEM)] and was outgrown by the P form [competitive index = 106.3 ± 26.6 (SD)] (fig. S8) after 24 hours of growth at 28°C in lysogeny broth plus sodium pyruvate (LBP). The

Fig. 2. Expression of the *mad* fimbrial locus and *madO* are required for M formation. (**A**) Physical map of the *mad* locus required for maternal adhesion, which is an initial step of nematode mutualism. *madA* to *K* are co-transcribed and expressed by inversion of the *madswitch* promoter located between *madR* and *madA*. *madR* is predicted to encode a FimB-type site-specific recombinase (i.e., invertase). (**B**) Expression of *mad* is essential for M formation. The majority of TT01 wild-type P-form cells switch to the M form 4 days after insect infection. Marked mutations (e.g., Δ*madA*::Gm^R) of *madA*, *H*, *J*, and an orphan FimB-type recombinase *madO* failed to switch to the M form at detectable levels. Δ*madR*::Gm^R switched to the M form. In-frame deletions in *madA* and *madH*, but not *madJ*, led to a switch to the M form. Error bars represent standard deviation. (**C** to **H**) (Left) Colonies 4 days after P-form infection of insects, except the locked strains (D and E); (right) selection of the M form during maternal adhesion in nematodes. (C) TT01 wild type switched to the M form in insects and in nematodes. (D) No M-form colonies (N = 883) and no maternal adhesion were detected in the locked L/P form. (E) Locked L/M form grew as M-form colonies (N = 1656) lacking sectors of the P form and adhering to the posterior nematode intestine. (F) Deleting the MadR invertase did not result in loss of switching to the M form in insects or nematodes. (G) Deleting the MadO invertase prevented switching to the M form in insects and nematodes. (H) Deleting MadJ resulted in no detectable M form in insects and 54% of maternal nematodes lacking adherent bacteria. i, intestine; r, rectum.
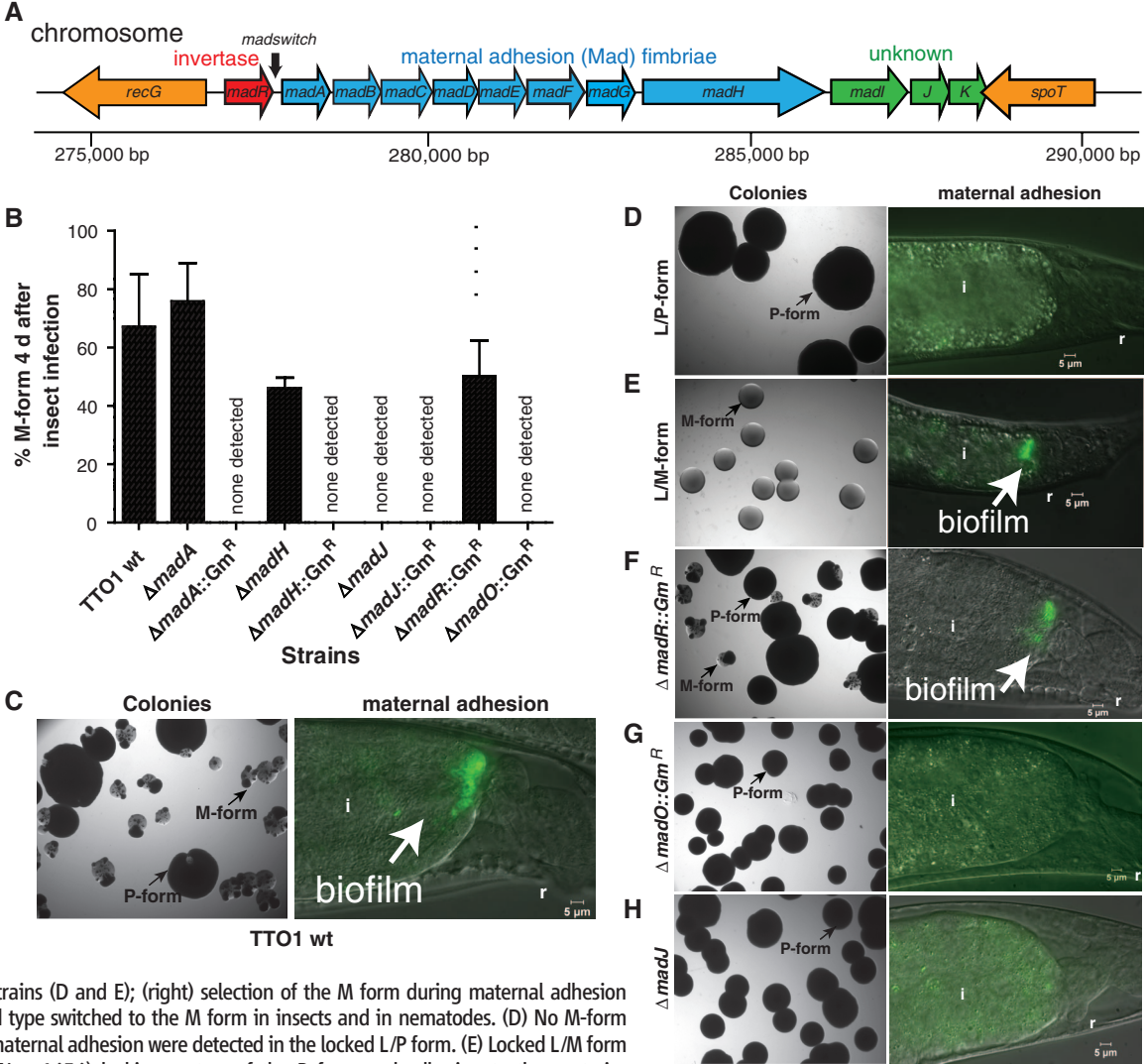
competitive disadvantage of the M form in co-culture was more than expected on the basis of the differences in growth rates. The M form produced less biofilm on polystyrene and was nonmotile (fig. S8). It also produced less bioluminescence, pigment, antibiotic, siderophore, and hemolysin (Fig. 3, A to E) and only minor amounts of rhabduscin, anthraquinone pigments,

and multipotent stilbenes (19). Stilbenes have been shown to act as antibiotics, insect phenoloxidase inhibitors, and nematode development signals (20, 21). All of these molecules were robustly produced by the P form (Fig. 3G). The M form produced more cinnamate, a precursor to stilbenes, after 48 hours of growth (fig. S9) likely because of less stilbene synthesis and

cinnamate hydrolysis (22, 23). IJ nematodes resumed development and reproduced less on the M form than on the P form (fig. S8). The M form had an altered capsule, absorbed less methylene blue and Congo red dyes, and exhibited a lower ability to reduce tetrazolium chloride dye (fig. S10). Finally, the M form was avirulent to insect *Galleria mellonella* larvae [time in which 50% of larvae die (LT_{50}) > 6 days, dose of ~100 cells] relative to the P form (LT_{50} < 2 days) (Fig. 3F). These radical differences likely reflect the dedicated function of each form (i.e., initiating nematode mutualism or insect pathogenicity).

Slow-growing small-colony variants and dormant persister cells are known to occur during chronic infections (24, 25). Because M forms emerge from prolonged aging of P-form colonies, we reasoned that the M form develops a higher incidence of persister cells (a high persister, *hip* phenotype). Indeed, the M form exhibited a *hip* phenotype, with >0.15% of cells tolerant to 1 µg/ml ciprofloxacin after 3 hours of exposure, which was 49.3 times the 0.003% tolerance of P-form cells ($P = 0.01$) (Fig. 3H). The M form also exhibited more (8.7-fold, $P = 0.005$) tolerance to streptomycin aminoglycoside antibiotic (fig. S11). This degree of resistance provides further evidence that the M form is biased toward dormancy, which could be advantageous inside the nematode.

Table 1. M formation, maternal adhesion, and transmission of *Photorhabdus mad* mutants. Column 1, M-form cells in insects 4 days after injection of P-form cells. Column 2, adhesion in the intestines of maternal nematodes at 38 to 40 hours; n = 40 to 60 animals. Column 3, transmission in the intestines of 7-day-old IJ offspring; n = 400 to 500 animals. All values ± standard deviation of the mean; ND, none detected.

| Strains	M form (%)	Maternal adhesion (%)	Percent transmission to IJs (%)
TT01 (wild type)	67.1 ± 18	98.4 ± 1.3	94.4 ± 2.9
L/P form	ND*	ND	ND
L/M form	100*	97.3 ± 1.6	92.1 ± 6.4
ΔmadR::GmR	50.2 ± 12.2	98.6 ± 1.9	90.6 ± 3.2
ΔmadA::GmR	ND	ND	ND
ΔmadA	75.8 ± 13.1	ND	ND
ΔmadH::GmR	ND	ND	ND
ΔmadH	46.0 ± 3.6	ND	ND
ΔmadJ::GmR	ND	41.4 ± 8.0	19.1 ± 3.5
ΔmadJ	ND	46.1 ± 8.0	21.5 ± 6.4
ΔmadO::GmR	ND	ND	ND

*Determined from colonies from an overnight liquid LBP culture; n = 883 for L/P form, n = 1656 for L/M form.
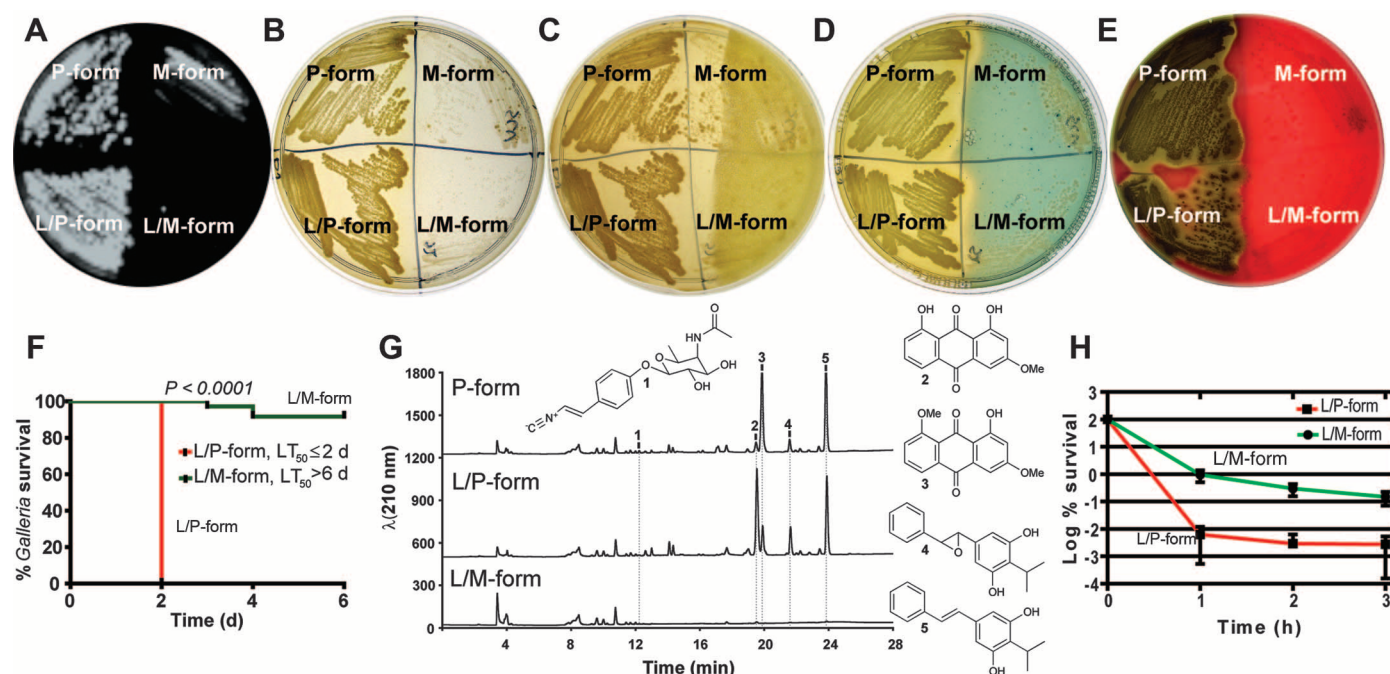
Fig. 3. Change in phenotypes, pathogenicity, secondary metabolite production, and persistence between P and M forms. (**A**) to (**E**) Quadrants on Petri dishes containing the P form (left), M form (right), unlocked forms (top), and locked forms (bottom). (A) Bioluminescence produced by the P form, which is absent in the M form (note that bioluminescence from P-form revertants is visible in the M form). (B) The P form is yellow and opaque, and the M form is unpigmented and transparent. (C) Antimicrobial activity produced at 48 hours of growth on LBP by the P form and not the M form against a soft-agar overlay containing *Micrococcus luteus* indicator bacteria. (D) Production of siderophore iron-chelating activity by the P form and not the M form indicated as a zone of clearing as iron is removed from chrome azural S chelator. (E) Hemolytic activity on sheep blood agar produced by the P form but not the M form. (**F**) Virulence of the L/P form and not the L/M form after injection into *Galleria mellonella*. (**G**) Metabolite analysis detected the production of rhabduscin (**1**), two anthraquinone pigment molecules (**2** and **3**) and two hydroxystilbene molecules (**4** and **5**), which were mostly absent in the L/M form. (**H**) There are 50 times more persister cells tolerant to ciprofloxacin in the L/M form than in the L/P form.
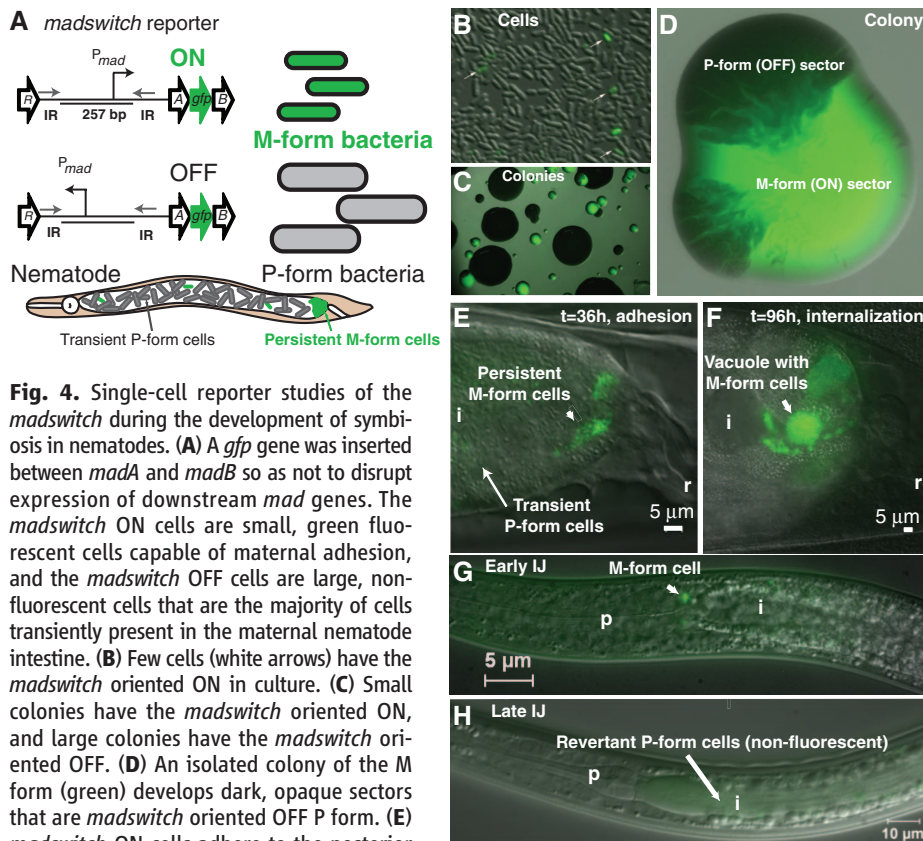
Fig. 4. Single-cell reporter studies of the *madswitch* during the development of symbiosis in nematodes. (**A**) A *gfp* gene was inserted between *madA* and *madB* so as not to disrupt expression of downstream *mad* genes. The *madswitch* ON cells are small, green fluorescent cells capable of maternal adhesion, and the *madswitch* OFF cells are large, nonfluorescent cells that are the majority of cells transiently present in the maternal nematode intestine. (**B**) Few cells (white arrows) have the *madswitch* oriented ON in culture. (**C**) Small colonies have the *madswitch* oriented ON, and large colonies have the *madswitch* oriented OFF. (**D**) An isolated colony of the M form (green) develops dark, opaque sectors that are *madswitch* oriented OFF P form. (**E**) *madswitch*-ON cells adhere to the posterior maternal nematode intestine, and most cells transiently present are not fluorescent, with the *madswitch* OFF. (**F**) Most adherent cells that invade and grow inside vacuoles of the rectal gland cells have the *madswitch* oriented ON. (**G**) One or two cells on or inside the pharyngeal intestinal valve cells have the *madswitch* oriented ON. (**H**) Seven days after the symbionts fully colonize the IJs, all cells are not fluorescent with the *madswitch* OFF, and again, the insect pathogenic P form is arming the nematode for insect infection. i, intestine; r rectum; p, pharynx.

Furthermore, comparison of the transcriptomes of the locked M and P forms revealed that >10% of the genome, or 250 up-regulated genes (≥2-fold, $P \le 0.05$) and 265 down-regulated genes (≤0.5-fold, $P \le 0.05$), was differentially expressed in LBP at 24 hours and 28°C (tables S1 and S2). One locus highly expressed in the L/M form was that of clustered regularly interspaced short palindromic repeats (CRISPR)–associated sequences (CASs), which may function in gene silencing with other CAS-CRISPR sequences (*26*) (table S1). Other strongly up-regulated genes included *madA*, which was validated by quantitative reverse transcription polymerase chain reaction (fig. S12), and *hexA*, which is known to repress P-form phenotypes (*27*). Notable down-regulated genes were those encoding CipA and CipB (*8*), luciferase, PrtA protease (*28*), and Tc insecticidal toxins (*5*) (tables S1 and S2). The down-regulation of genes involved in heme and menaquinone biosynthesis (*hemD*, *hemE*, *menA*, *aroF*, and *aroQ*) indicates a reduced electron potential in the M form, like that of many clinical small-colony variants (*24*) (table S2).

In organisms that switch between phenotypic variants, analogous to cooperating and cheating,

the abundance of each type is a result of switching frequencies and variant fitness (*29*). The P to M form switching frequency (1.21×10^{-3} per cell per generation) was greater than the M to P form switching frequency (4.30×10^{-5} per cell per generation), which indicated that, although the P form switches to the M form 28 times more often than the reverse, the superior fitness of the P form enables it to remain dominant in culture (fig. S8). The higher fitness of the P form explains why M-form colonies are overtaken by the P form and why P-form colonies remain P-form colonies during laboratory growth (i.e., LBP, at 28°C, for 48 hours).

To visualize M formation at single-cell resolution, a green fluorescent protein *gfp* reporter was inserted between *madA* and *madB* (Fig. 4A). Few M-form cells were present in culture, and the resultant M-form colonies developed nonfluorescent sectors of P-form revertants (Fig. 4, B to D). Cells initiating nematode mutualism were green, whereas most cells transiently present in the nematode intestine were not (Fig. 4E). The M form prevailed during intracellular growth and the initial step of IJ colonization (Fig. 4, F and G). However, bacterial cells in the fully colonized IJ

intestine were not green and grew mostly as P-form colonies, which indicated that the IJs had become armed with the P form (Fig. 4, H and I, and fig. S13). Because the MadO invertase is required to flip the *madswitch* from OFF to ON, repressing MadO in IJ cells may favor MadR flipping of the *madswitch* from ON to OFF (fig. S1). Data supporting this model include the observation that 92.5% of colonies from IJs colonized by the $\Delta madR::Gm^R$ mutant were the M form, whereas only 0.29% were M form from IJs associated with P form (fig. S13).

Our examination of a multipartite interaction among bacteria, nematodes, and insects in a tractable model system provides key molecular insight into the drivers of phenotypic behaviors of *Photorhabdus* bacteria in their nematode and insect hosts. A stochastic promoter inversion switch controls the bacterial phenotypes, i.e., the M-form and P-form variants with dramatically different physiologies, required for initiating mutualistic or pathogenic life-styles, respectively. During initiation of nematode mutualism, most cells inside the maternal nematode intestine were P-form transients, but although fewer M-form cells persisted, they were preferentially transmitted to IJ offspring developing inside the maternal nematode. However, bacterial cells in fully colonized IJs switched back to the P form and armed these nematodes for insect infection. Chance promoter inversion appears to be an efficient mechanism in *Photorhabdus* to reversibly switch between conflict and cooperation with two different animal hosts.

References and Notes

1. E. R. Moxon, P. B. Rainey, M. A. Nowak, R. E. Lenski, *Curr. Biol.* **4**, 24 (1994).
2. N. Q. Balaban, J. Merrin, R. Chait, L. Kowalik, S. Leibler, *Science* **305**, 1622 (2004).
3. T. A. Ciche, J. C. Ensign, *Appl. Environ. Microbiol.* **69**, 1890 (2003).
4. N. R. Waterfield, T. Ciche, D. Clarke, *Annu. Rev. Microbiol.* **63**, 557 (2009).
5. D. J. Bowen, J. C. Ensign, *Appl. Environ. Microbiol.* **64**, 3029 (1998).
6. D. Bowen *et al.*, *Science* **280**, 2129 (1998).
7. P. J. Daborn *et al.*, *Proc. Natl. Acad. Sci. U.S.A.* **99**, 10742 (2002).
8. S. B. Bintrim, J. C. Ensign, *J. Bacteriol.* **180**, 1261 (1998).
9. W. H. Richardson, T. M. Schmidt, K. H. Nealson, *Appl. Environ. Microbiol.* **54**, 1602 (1988).
10. T. A. Ciche, K. S. Kim, B. Kaufmann-Daszczuk, K. C. Nguyen, D. H. Hall, *Appl. Environ. Microbiol.* **74**, 2275 (2008).
11. V. S. Somvanshi, B. Kaufmann-Daszczuk, K. S. Kim, S. Mallon, T. A. Ciche, *Mol. Microbiol.* **77**, 1021 (2010).
12. S. P. Nuccio, A. J. Bäumler, *Microbiol. Mol. Biol. Rev.* **71**, 551 (2007).
13. R. E. Hurlbert, J. Xu, C. L. Small, *Appl. Environ. Microbiol.* **55**, 1136 (1989).
14. R. J. Akhurst, *J. Gen. Microbiol.* **121**, 303 (1980).
15. J. Zieg, M. Hilmen, M. Simon, *Cell* **15**, 237 (1978).
16. M. W. van der Woude, A. J. Bäumler, *Clin. Microbiol. Rev.* **17**, 581 (2004).
17. K. Eichler, A. Buchet, R. Lemke, H. P. Kleber, M. A. Mandrand-Berthelot, *J. Bacteriol.* **178**, 1248 (1996).
18. W. Deng *et al.*, *Proc. Natl. Acad. Sci. U.S.A.* **101**, 3597 (2004).
19. J. M. Crawford, R. Kontnik, J. Clardy, *Curr. Biol.* **20**, 69 (2010).

20. S. A. Joyce *et al.*, *Angew. Chem. Int. Ed. Engl.* **47**, 1942 (2008).
21. I. Eleftherianos *et al.*, *Proc. Natl. Acad. Sci. U.S.A.* **104**, 2419 (2007).
22. J. S. Williams, M. Thomas, D. J. Clarke, *Microbiology* **151**, 2543 (2005).
23. S. Chalabaev *et al.*, *Appl. Environ. Microbiol.* **74**, 1717 (2008).
24. R. A. Proctor *et al.*, *Nat. Rev. Microbiol.* **4**, 295 (2006).
25. K. Lewis, *Annu. Rev. Microbiol.* **64**, 357 (2010).
26. K. S. Makarova *et al.*, *Nat. Rev. Microbiol.* **9**, 467 (2011).
27. S. A. Joyce, D. J. Clarke, *Mol. Microbiol.* **47**, 1445 (2003).
28. D. J. Bowen *et al.*, *Microbiology* **149**, 1581 (2003).
29. M. Acar, J. T. Mettetal, A. van Oudenaarden, *Nat. Genet.* **40**, 471 (2008).
30. R. Edgar, M. Domrachev, A. E. Lash, *Nucleic Acids Res.* **30**, 207 (2002).

Identification and Functional Expression of the Mitochondrial Pyruvate Carrier

Sébastien Herzig,[1] Etienne Raemy,[1] Sylvie Montessuit,[1] Jean-Luc Veuthey,[2] Nicola Zamboni,[3] Benedikt Westermann,[4] Edmund R. S. Kunji,[5] Jean-Claude Martinou[1]*

The transport of pyruvate, the end product of glycolysis, into mitochondria is an essential process that provides the organelle with a major oxidative fuel. Although the existence of a specific mitochondrial pyruvate carrier (MPC) has been anticipated, its molecular identity remained unknown. We report that MPC is a heterocomplex formed by two members of a family of previously uncharacterized membrane proteins that are conserved from yeast to mammals. Members of the MPC family were found in the inner mitochondrial membrane, and yeast mutants lacking MPC proteins showed severe defects in mitochondrial pyruvate uptake. Coexpression of mouse MPC1 and MPC2 in *Lactococcus lactis* promoted transport of pyruvate across the membrane. These observations firmly establish these proteins as essential components of the MPC.

In the mitochondrion, pyruvate is converted into acetyl–coenzyme A (acetyl-CoA) by the pyruvate dehydrogenase (PDH) complex and participates in the synthesis of branched-chain amino acids (BCAAs) in yeast. Acetyl-CoA donates carbon atoms to the citric acid cycle and participates in the synthesis of octanoic acid, the precursor of lipoic acid (*1*). Lipoic acid is an essential cofactor of several multi-subunit complexes in the mitochondrial matrix, including PDH, α-ketoglutarate dehydrogenase (α-KDH), and the branched-chain keto acid dehydrogenase (BCKDH) (*2*). Import of pyruvate across the inner mitochondrial membrane (IMM) requires a specific carrier whose molecular identity has not been established (*3*). We have identified a family of membrane proteins (pfam UPF0041) whose members are necessary and sufficient for the transport of pyruvate into mitochondria. We have renamed this family the mitochondrial pyruvate carrier (MPC) family.

We previously identified MPC1 (formerly Brp44L) in a proteomic analysis of the IMM of mouse liver (*4*). MPC1 and its paralog MPC2 (formerly Brp44) have unknown function. Both are IMM proteins with three predicted transmembrane α-helices on the basis of secondary structure predictions and hydropathy profiling (fig. S1). They share sequence similarity with yeast Mpc1 (Ygl080w), Mpc2 (Yhr162w), and Mpc3 (Ygr243w) (fig. S1, C and D). We used *Saccharomyces cerevisiae* as a model organism to investigate the function of this family of proteins.

In yeast, Mpc1 localized in the IMM (fig. S2). Growth of the knockout mutants *mpc1Δ*, *mpc2Δ*, *mpc3Δ*, and *mpc2Δmpc3Δ* was normal on rich medium, either containing fermentable [yeast extract, peptone, and dextrose (YPD)] or nonfermentable carbon sources [Yeast extract, peptone, glycerol (YPG)] (Fig. 1A). In contrast, *mpc1Δ* and *mpc2Δ mpc3Δ* cells grew more slowly in amino acid–free medium [synthetic dextrose (SD)] than did the cells of the isogenic wild-type (WT) strain (Fig. 1A and fig. S3A). Deletion of *MPC2* alone led to a minor growth defect, whereas deletion of *MPC3* had no visible effect on growth. A similar phenotype was observed by (*5*). Expression of WT *MPC1* restored growth of *mpc1Δ* cells (Fig. 1, B and C). Suppressor screens for genes that restored growth of *mpc1Δ* cells in SD identified only *MPC1* (supplementary text),

suggesting that its function cannot be complemented by other genes. Expression of either *MPC2* or *MPC3* restored growth of *mpc2Δmpc3Δ* cells but not that of cells lacking *MPC1* (Fig. 1, B and C). Thus, the growth of yeast in SD required a combination of Mpc1 with Mpc2 or Mpc3. We found that Mpc1 coimmunoprecipitated with Mpc2, suggesting that they form a heterocomplex (fig. S3B).

The growth defect in SD was relieved by addition of valine or leucine, with an additive effect of both amino acids (Fig. 1A). In contrast, addition of all amino acids except leucine and valine did not restore growth of the mutant strains (SC –V –L) (Fig. 1A). This finding prompted us to investigate the role of MPC proteins in the metabolism of valine and leucine. We assayed their decarboxylation by monitoring the release of $^{14}CO_2$ by cells grown in SD supplemented with either 1-^{14}C valine or 1-^{14}C leucine. Release of $^{14}CO_2$ by *mpc1Δ* cells was less than 2% of that in WT cells (Fig. 1D). A similar defect occurs in a *lpd1Δ* strain (Fig. 1E) (*6*), lacking a lipoamide dehydrogenase essential for the function of the mitochondrial dehydrogenase complexes, PDH, α-KDH (*7*), and BCKDH (*8*). To test whether *mpc1Δ* cells also had dysfunctional PDH and α-KDH, we assessed their activities in mitochondria. The activity of these two complexes was impaired in mitochondria from *mpc1Δ* cells grown in SD (Fig. 1F), suggesting that the function of Mpc1 extends to several lipoyl-dependent complexes.

Lipoic acid is covalently attached to the E2 subunits of PDH (Lat1) and α-KDH (Kgd2), the E3-binding protein of PDH (Pdx1), and the H subunit of the glycine cleavage system (Gcv3) (*9*, *10*). This modification can be readily assessed by means of protein immunoblotting with antibodies to lipoic acid (*11*). In rich medium, WT, *mpc1Δ*, *mpc2Δ*, *mpc3Δ*, and *mpc2Δmpc3Δ* cells had similar amounts of lipoylated complexes (Fig. 2A). However, when cells were grown in SD, lipoylated proteins were virtually absent from *mpc1Δ*, *mpc2Δ*, and *mpc2Δmpc3Δ* but not *mpc3Δ* cell lysates (Fig. 2A). Addition of valine or leucine, or both, to SD or expression of *MPC1* restored lipoylation in *mpc1Δ* (Fig. 2B and fig. S3C). The defect in lipoylation was correlated with decreased abundance of lipoic acid in *mpc1Δ* cells grown in SD (fig. S3D). In contrast, lipoic

[1]Department of Cell Biology, University of Geneva, 1211 Geneva 4, Switzerland. [2]School of Pharmaceutical Sciences, University of Geneva, 1211 Geneva 4, Switzerland. [3]Institute of Molecular Systems Biology, 8093 Zurich, Switzerland. [4]Zellbiologie, Universität Bayreuth, 95440 Bayreuth, Germany. [5]Mitochondrial Biology Unit, Medical Research Council, Cambridge CB2 0XY, UK.

*To whom correspondence should be addressed. E-mail: jean-claude.martinou@unige.ch

Science

A Single Promoter Inversion Switches *Photorhabdus* Between Pathogenic and Mutualistic States

Vishal S. Somvanshi, Rudolph E. Sloup, Jason M. Crawford, Alexander R. Martin, Anthony J. Heidt, Kwi-suk Kim, Jon Clardy and Todd A. Ciche

Twin Tales of Two Toxins

The luminescent bacterium, *Photorhabdus luminescens*, is carried in the gut of an insect-parasitic nematode as a stealth weapon. By using an allele swapping technique, **Somvanshi** *et al.* (p. 88) investigated the promoter-switching mechanism that flips the bacterium from the almost dormant M forms, which stick to the adult nematode's posterior gut, into the motile, luminous P forms, which are armed with the toxic virulence factors needed to overcome the insect prey of the nematode. Similar switches may operate in bacteria that flip between harmless commensals and lethal pathogens. The bio-control agent *Bacillus thuringiensis* also kills insects by means of a crystal toxin, which allows the bacteria to penetrate the host gut and access nutrients. Release of nutrients also allows bacterial cheats that do not make toxin, to grow and outcompete the toxin-producing colonizers. In field experiments, **Raymond** *et al.* (p. 85) found that, consequently, the bacterial population becomes less virulent. Because these type of virulence factors are secreted from the cell and are widespread in pathogens, such social interactions may affect the fitness and constrain the virulence of many toxin-producing bacteria.